Journal of Materials Chemistry B

Accepted Manuscript

ROYAL SOCIETY OF CHEMISTRY

www.rsc.org/materialsB

Journal of Materials Chemistry B RSCPublishing

ARTICLE

Substrate independent coating formation and anti-biofouling performance improvement of mussel inspired polydopamine

Cite this: DOI: 10.1039/x0xx00000x

Received 00th January 2012,
Accepted 00th January 2012

DOI: 10.1039/x0xx00000x

www.rsc.org/

Yuan Dang, Cheng-Mei Xing, Miao Quan, Yan-Bing Wang, Shi-Ping Zhang, Su-Qing Shi and Yong-Kuan Gong*

Mussel inspired polydopamine (PDA) coating has been proven to be a simple and effective method for surface modification of biomaterials. However, the adhesive functional groups remaining on the surface of PDA coating may promote the attachment of nonspecific protein and microorganism and hinder anti-biofouling performance. In this study, the PDA coating formation process is monitored in real-time by a sensitive surface plasmon resonance (SPR) technique under different pH, initial dopamine concentration and deposition time. The coating morphology is observed by atomic force microscopy (AFM). Nonspecific protein adsorption, platelet and fibroblast cell adhesion, as well as bacteria attachment on the PDA coatings of different thicknesses are measured to evaluate their anti-biofouling performance. Thickness-dependent biofouling of the PDA coatings is demonstrated due to the accumulation of adhesive functional groups within the PDA matrix. In order to reduce the biofouling, we treat the PDA coating by $FeCl_3$ coordination, $NaIO_4$ oxidation, heating in air and grafting with a phosphorylcholine copolymer bearing active ester groups. The modified surfaces are characterized by X-ray photoelectron spectra (XPS) and attenuated total reflection Fourier transform infrared (ATR-FTIR) spectroscopy measurements. Interestingly, all the treatments help to resist protein adsorption significantly. More excitingly, the simple grafting strategy with phosphorylcholine copolymer can resist more than 99% of platelet, fibroblast, and bacteria cell attachment, 98% of bovine serum albumin and 95% of bovine plasma fibrinogen adsorption on the PDA coating. These results may find applications in the vast area of surface antifouling, especially for most biomedical devices.

1 Introduction

Biofouling is a universal problem caused by nonspecific protein, cell or microorganism attachment on surfaces in various applications ranging from membrane systems, ship hulls to implantable biomedical devices. For example, biofouling degrades the performance of surface-based diagnostic devices, causes an adverse effect on the healing process for implanted biomaterials and is believed to be a major cause of mortality.[1,2] Consequently, numerous surface modification strategies have been developed, such as plasma polymerization, polymer coating, nanoparticle immobilization, conjugation of bioactive molecules, and layer-by-layer self-assembly[3-9].

Excellent anti-biofouling performance has been observed on hydrophilic polymer surfaces such as poly(ethylene glycol)[10,11] and zwitterionic polymers including poly(carboxybetaine),[12-14] poly(sulfobetaine)[15-17] and poly(2-methacryloyloxyethyl phosphorylcholine)[18,19]. However, these polymers are extremely hydrophilic and hence have high solubility in water, making them difficult to be attached onto a surface. Therefore, specific interaction between the polymer and the substrate surface is required to immobilize such hydrophilic polymers. Unfortunately, most substrates such as plastics, metals, and ceramics commonly have inert surfaces and are difficult to be modified. The lack of a simple and inexpensive coating approach has been the major obstacle for practical implementation.

Inspired by the bio-adhesion principle of marine mussels in wet and turbulent environments, Messersmith and his colleagues found that dopamine could spontaneously polymerize under slightly alkaline conditions, leading to the formation of a polydopamine (PDA) coating with secondary reactivity on virtually all substrates[20]. Although the exact mechanism of PDA coating formation and adhesion remains elusive, there is a general acceptance that the catechol group plays the central role in such mussel-mimicking versatility.[21,22]

The polymerization of dopamine needs to be initiated by an oxidization reaction.[20,23,24]

The molecular mechanism of PDA formation has long been debated due to the complex redox process as well as the generation of a series of intermediates during the polymerization and reaction processes.[2] Lee and co-workers suggested that the formation of PDA was a result of the combination of covalent polymerization and noncovalent self-assembly.[25] The covalent-bond interaction plays a critical role during the initial steps of PDA buildup, while noncovalent bond interactions play a greater role after the oligomerization reaction has proceeded significantly. Consequently, many functional groups including planar indole units, amino group, carboxylic acid group, catechol or quinone functions, and indolic/catecholic π-systems are integrated into PDA, which may specifically explain the robust adhesion capability of PDA to virtually all types of surfaces, and also provide a versatile platform for further conjugation of interesting functionalities.[2] The interactions of PDA with substrates include covalent binding and noncovalent binding, and are varied depending on the surface properties of the substrates. The covalent binding mechanism is applicable to some specific substrates that contain amine and/or thiol groups on their surfaces via Michael addition and/or Schiff-base reactions under basic conditions. On the other hand, PDA, similar to its monomer, is prone to attachment on substrates through noncovalent binding interactions such as metal coordination, hydrogen bonding, π−π stacking, and quinhydrone charge-transfer complexes to yield a robust coating.[26,27]

Due to its simplicity and good biocompatibility, PDA coating has recently attracted great interest and was intensively studied for surface modification of biomaterials.[2,23,28-31] As a major component of naturally occurring melanin that is widely distributed in human body, PDA is anticipated to show excellent biocompatibility. The possible toxicity of PDA was initially studied in vitro by Park's group. Fibroblasts, osteoblasts, neurons, and endothelial cells cultured on PDA coated various substrates showed normal proliferation without cytotoxicity[32,33]. In vivo toxicity evaluation of PDA coating was reported by Hong *et al* on quantum dots (QDs) and PLLA films.[34] Using mice models, it was shown that the PDA coating reduced the blood toxicity of semiconductor QDs and the inflammatory reactions of PLLA. The PDA coated nanoparticles showed a relatively high LD_{50} in rats and all of the treated animals remained healthy within a period of 1 month after intravenous administration. The histopathological examination of several organs revealed a normal parenchymal architecture without any tissue damage, inflammatory, or fibrosis aspect with no detectable change in the cellular structures, suggesting an effective strategy to form ultrastable coatings on nanoparticles in vivo with improved biocompatibility.[35,36] In addition, PDA coated reverse osmosis and ultrafiltration membranes not only retained much of the membranes' intrinsic pure water permeability, but also improved their fouling resistance.[37,38]

However, Huang's group demonstrated that PDA modified TiO_2 nanotubes and 316L stainless steel promoted Fg and thrombin adsorption and triggered severe platelet activation and red blood cell aggregation. Moreover, obvious enhancement of cell adhesion, growth and spreading on PDA surface was found.[39-41] In line with Huang's results, Park *et al* reported that substrates with PDA coating promoted the adhesion of many kinds of mammalian cells.[32,33] They explained that the increase of cell adhesion on PDA-coated surfaces was attributed to the adsorption of proteins on PDA layer by the reaction with amine- or thiol- functionalized molecules via Schiff-base or Michael addition chemistry. In our previous report, catechol content in phosphorylcholine and catechol grafted 8-arm PEG coatings was closely related to the attachment of protein, platelet, fibroblast cell and bacteria.[42] The aforementioned results suggested that the versatile adhesion property of PDA might bring considerable attachment of biofoulants. Therefore, we questioned whether the pristine dip-coated PDA coating could be directly utilized as a surface modifier for blood-contacting or anti-biofouling devices. Surprisingly, less effort has been devoted to the systematic investigation of PDA coating formation and the anti-biofouling performance.

Herein, different thicknesses of PDA coatings were fabricated on surface plasmon resonance (SPR) sensor chips and other substrates under different conditions to have better insights into the deposition process of PDA coating. Protein adsorption, platelet, L929 fibroblast cells and bacteria adhesion on PDA coatings of gradient thicknesses were subsequently measured to correlate the anti-biofouling performance with the PDA-thickness. Furthermore, the PDA coatings were treated by $FeCl_3$ coordination, $NaIO_4$ oxidation, heating and grafting with a cell membrane mimetic phosphorylcholine copolymer. The anti-biofouling performance of the differently treated coatings was evaluated systematically. Overall, this work demonstrated that the anti-biofouling performance of PDA coating is limited and can be improved significantly by the simple treatments.

2 Materials and methods

2.1 Materials

3-Hydroxytyramine hydrochloride (dopamine), bovine serum albumin (BSA), and bovine plasma fibrinogen (Fg) were purchased from Sigma-Aldrich and used as received. 2-Methacryloxoethyl phosphorylcholine (MPC) and *p*-nitrophenoxycarbonyloxyethyl methacrylate (NPCEMA) were synthesized according to the methods reported by Ishihara[43] and Konno[44]. A random copolymer bearing phosphorylcholine and active ester groups (PMEN) was synthesized using monomers of MPC and NPCEMA according to the reported method[45]. The chemical structure and ^{1}H NMR spectrum of PMEN copolymer was shown in Fig. S1. Water used was purified using a Millipore water purification system with a minimum resistivity of 18.2 MΩ·cm. All other chemicals were analytical reagents grade and were used without further purification unless otherwise indicated.

2.2 PDA coating fabrication on SPR sensor chips

PDA coating deposition process was monitored on a Reichert SR7500DC dual channel SPR system (Reichert, USA). The bare gold chip was firstly attached to the base of the prism. Optical contact between two surfaces was realized using a refractive index matching fluid (Cargille). Dopamine was dissolved in 10 mM Tris/HCl buffer just before the beginning of each deposition experiment. The fabrication procedure of PDA coating was conducted as the following protocol with a flow rate of 10 μl/min at 25 ℃: (a) passing the degassed 10 mM Tris/HCl buffer over the chip for at least 10 min to obtain a stable baseline; (b) delivering dopamine solution over the gold surface for the specified time; (c) then rinsing the surface with the buffer for about 30 min to wash off the loosely combined dopamine. The quantity of the adsorbed/adhered PDA was evaluated by the baseline difference given in response units before and after injecting the dopamine solution.

Dopamine solutions with different concentration, pH and deposition time were designed to control the PDA film formation.

2.3 Modification of PDA coating

Modification treatments of the PDA coated chips were processed individually as follows: (1) injecting 0.01 mg/ml $FeCl_3$ aqueous solution through the PDA coated SPR chips at a flow rate of 5 μl/min for specific periods, (2) injecting 0.01 mg/ml $NaIO_4$ aqueous solution over the PDA coated SPR chips at a flow rate of 5 μl/min for specific periods, (3) 130 ℃ heating the PDA coated chips in air for different times, (4) injecting PMEN polymer solution through the PDA coated gold chips at a flow rate of 5 μl/min for specific periods. The modified PDA coatings were used for further characterizations after washing with PBS buffer or water.

The pristine or modified PDA coatings on other substrates were prepared in a way similar to the fabrication process on the gold chip surface.

2.4 Attenuated total reflection Fourier transform infrared spectroscopy (ATR-FTIR)

PDA coated polypropylene (PP) and bare PP were employed to measure the ATR-FTIR by a Fourier transform infrared (FTIR) spectrometer (Spectrum Two, PerkinElmer Corporation, USA) equipped with a diamond universal ATR. The spectra were recorded at room temperature in the range 4000-450 cm^{-1} at a resolution of 1 cm^{-1} and the background spectra were recorded in air.

2.5 Surface elemental analysis

The elemental composition of the PDA coatings was determined by X-ray photoelectron spectroscopy (XPS) (K-Alpha, Thermo Electron Corporation, USA). All spectra were collected at an electron take-off angle of 90 ° from the surface under vacuum. Binding energies were calibrated relative to the C1s peak (284.8 eV) from hydrocarbons adsorbed on the surface of the samples. The high-resolution C1s, N1s and P2p spectra were fitted using a Shirley background subtraction and a series of Gaussian peaks using the XPSPEAK software.

2.6 Morphology characterization

Atomic force microscopy (AFM) measurement was performed on PDA deposited silicon wafers after rinsing with water and extensive drying under a stream of nitrogen. The morphological analysis of the studied surfaces was performed using a Multi Mode 8 AFM (Bruker Corporation, USA). A silicon tip on nitride cantilever from Bruker was utilized with Tapping Mode in air. The spring constant (k) was 40 N/m. The sample was attached to the magnetic stainless steel disc which was immobilized on the AFM machine without movement. 1×1 μm^2 randomly chosen areas were scanned at a scan frequency of 1 Hz using a 10×10 μm^2 type piezo scanner to understand the topography of the surfaces. The roughness of the surfaces was assessed by measuring roughness parameters, R_q (root mean square roughness).

2.7 Protein adsorption on PDA or modified PDA coatings

The representative proteins, BSA and Fg, were selected to study the protein adsorption performance of the specified surface using SPR method. The experiment was started by replacing 10 mM PBS (pH 7.4) buffer with 1.0 mg/ml BSA or Fg in the PBS buffer. After injecting for 10 min at the flow rate of 50 μl/ml, the protein solution was replaced with the PBS buffer. The amount of adsorbed proteins was expressed as the difference in response unit (μRIU) measured in PBS solution before and after contact with the proteins solution.

2.8 Platelet attachment

Platelet attachment test was performed under static conditions.[46] The coatings were placed in petri dishes and equilibrated by immersion in PBS for 2 hours. Subsequently, 20 μl fresh platelet-rich plasma (PRP) was added and incubated at 37 ℃ for 2 hours. Afterwards, the samples were rinsed with PBS to remove the weakly adhered platelets and the remaining adhered platelets are fixed in 2.5 wt% glutaraldehyde solution for 1 hour. After rinsing several times with PBS solution and Millipore water, the fixed samples were lyophilized overnight and observed with an FEI QUANTA 600 FEG SEM. At least three randomly chosen sections were captured and statistically analyzed by threshold analysis in ImageJ.

2.9 L929 cell adhesion

Cell adhesion test was performed using L929 cells. The coatings were placed in 24-well culture plates, sterilized and equilibrated in PBS. Then freshly harvested L929 mammalian fibroblast cells were resuspended in Dulbecco's Modified Eagle Media (DMEM) supplemented with 10% Fetal Bovine Serum (FBS) and 100 U/ml of penicillin/streptomycin at a concentration of 5×10^4 cells/ml. Afterwards, 2 ml/well L929 fibroblast cells suspension was added to replace PBS. The surfaces were then incubated at 37 ℃ and 5% CO_2 for 24 hours. Subsequently, PBS was used to rinse the substrates to remove any non-adherent cells. The adhered fibroblasts were stained

with 20 µl/well Syto9 in PBS (2 µl/ml) for 20 min and the samples were transferred to new culture plates with PBS buffer. Three random locations on each surface were captured using inverted fluorescence microscope (Ti-U, Nikon) and quantified by threshold analysis in ImageJ.

2.10 Bacteria adhesion

Bacteria adhesion on the coatings was assessed by Gram negative *Escherichia coli* (*E. coli*) and Gram positive *Staphylococcus aureus* (*S. aureus*) attachments from a suspension of 5×10^7 cells/ml in PBS. The attached bacteria were evaluated by fluorescent staining according to the method of Fullenkamp *et al.*[47] The coatings on glass substrates (10×10 mm^2) were placed into 24-well cell culture plates, sterilized by exposure to UV light for 30 min and then equilibrated with sterilized PBS for 2 hours. After replacing the PBS with the freshly prepared bacteria suspension, the samples were incubated at 37 ℃ for 24 hours. The surfaces were rinsed with PBS to remove loosely adhered bacteria. The attached bacteria were then stained with Syto9 (2 µl/ml) in PBS and visualized using an Olympus FV1000 confocal laser scanning microscopy (CLSM, with a 20× objective lens). Three identical surfaces for each experiment were analyzed for statistical purposes by threshold analysis in ImageJ.

3 Results and discussion

3.1 PDA coating formation

The PDA coating formation process was investigated by SPR real-time measurements under three circumstances.

The SPR response signals obtained after the injection of dopamine solutions with different pH were converted to the thickness of PDA coating (1 µRIU = 0.1 ng/cm^2, assuming a density of 1.0 g/cm^3 for the PDA polymer[48]) and the corresponding thickness sensorgrams were shown in Fig. 1. The increase in coating thickness with deposition time indicated that PDA film was deposited as time progressed. The slope of the PDA deposition sensorgram increased markedly when the pH

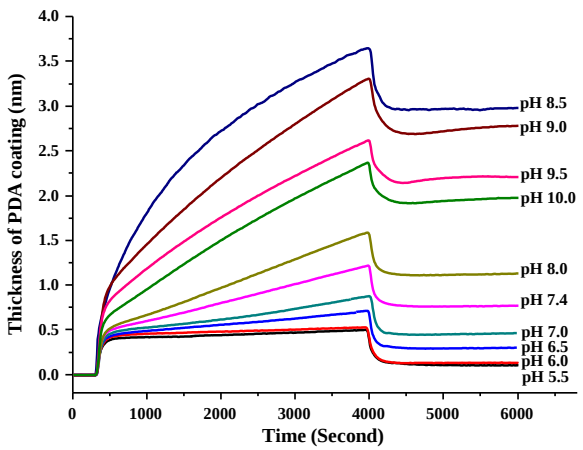

Fig. 1 SPR sensorgrams of PDA coating formation from 2 mg/ml dopamine solutions with different pH.

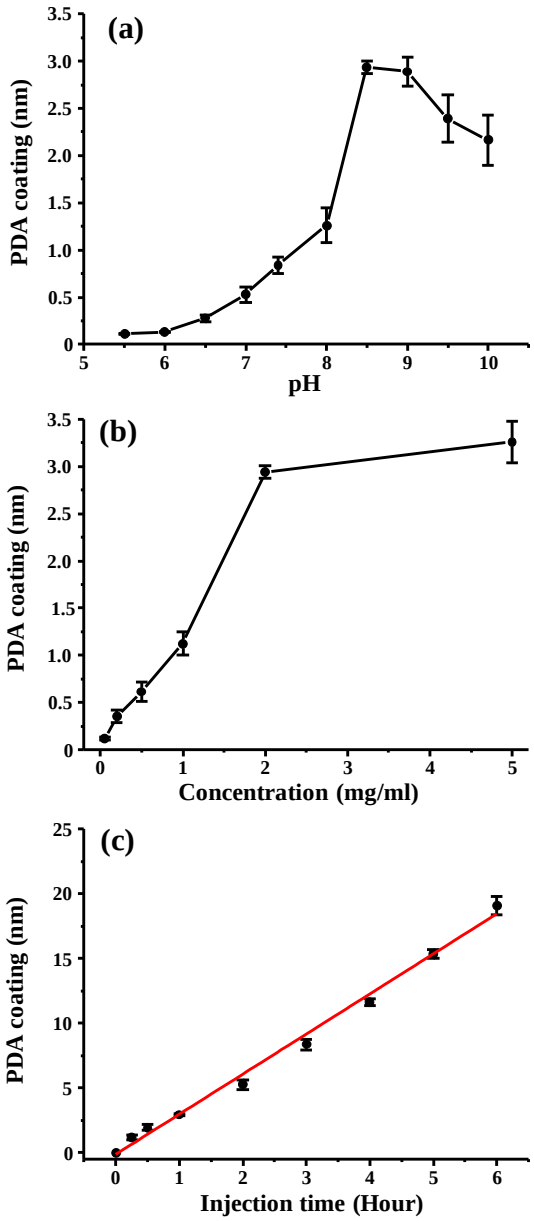

Fig. 2 Representative SPR results of PDA coating formation from dopamine aqueous solutions. (a) Effect of dopamine solution pH on PDA thickness at constant dopamine concentration of 2 mg/ml and deposition time of 1 hour. (b) Effect of dopamine concentration on PDA thickness at constant pH of 8.5 and deposition time of 1 hour. (c) Effect of injection time on PDA thickness at constant dopamine concentration of 2 mg/ml and pH of 8.5.

of dopamine solution was increasing from 6 to 8.5, suggesting a thicker PDA coating formation in more basic solution. Effect of dopamine solution pH on the PDA coating formation was demonstrated more clearly by plot of pH versus the thickness of PDA coating. As illustrated in Fig. 2(a), the deposited PDA film reached the maximal thickness at the pH of 8.5, suggesting a pH dependent coating formation process initialized by automatic oxidation in air.[42] When the pH exceeded 8.5, the PDA thickness decreased with increasing pH value and this phenomenon was in accordance with the report of Ball *et al.*[49] This result might be related to the rapid formation of large

aggregates in the solution and result in the shortage of unoxidized or partially oxidized dopamine for PDA coating formation and growth.[50] In Ball's investigation, they also confirmed that large PDA aggregates presented in solution did not contribute to the film deposition.

As shown in Fig. 2(b), the initial concentration of dopamine solution had a marked effect on the PDA film deposition. For the 1 hour deposition period, the thickness of deposited PDA coating was strongly dependent on the initial dopamine concentration, with increased coating thickness being obtained with increasing initial dopamine concentration. Under alkaline conditions (pH 8.5) with abundant oxygen as the oxidant, the increasing content of free dopamine in the initial solution was accompanied by the growing number of intermediates participating in the polymerization of dopamine, such as partly-oxidized dopamine or small oligomers. During the SPR operation, oxygen (about 10^{-3} mol/l at 25°C in water) in the mobile phase (Tris/HCl) is limited and thus may restrict the content of the oxidized intermediate within the dopamine solution. When the concentration of dopamine monomer was lower than 2 mg/ml, the thickness of PDA film increased rapidly with the growing number of dopamine, suggesting sufficient amount of oxygen in the solution for the oxidation reaction. Nevertheless, the thickness of deposited PDA showed little increase after the concentration of dopamine was higher than 2 mg/ml for the insufficient intermediate to satisfy the further coating growth. It is likely that the oxidation rate limited the polymerization rate in this experiment.

The relationship between PDA film thickness and deposition time was investigated by passing 2 mg/ml dopamine in 10 mM Tris/HCl (pH 8.5) buffer through the SPR chip for the specific time. Restricted by the detection range of the SPR instrument, we could only get the deposition information of PDA within 6 hours, as shown in Fig. 2(c). In our study period, the PDA thickness scaled linearly with the deposition time and the increasing tendency was found to agree well with the one reported by Lee *et al.*[20] After injecting dopamine Tris/HCl (pH 8.5) solution for 6 hours, the thickness of PDA coating was around 20 nm as calculated from the SPR response. This thickness measured by SPR method was slightly less than Lee's thickness value obtained by AFM. This systematic difference is not surprising for two reasons: (i) SPR monitors the absolute mass of the deposited PDA; (ii) The films used for the AFM measurements might be partially hydrated and swelling.[42] The thickness of PDA film can be well controlled by tuning the initial concentration and pH of the dopamine solution and as well as the polymerization time.

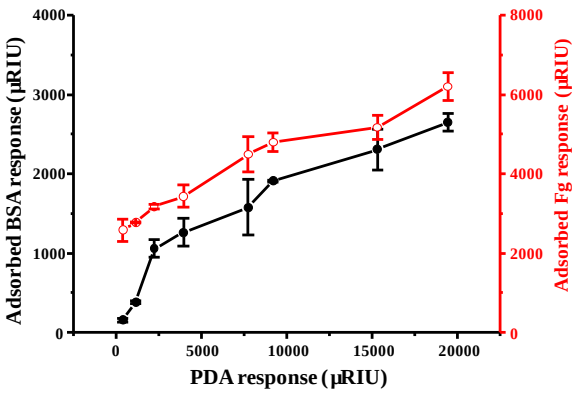

Fig. 3 Plots of SPR responses from BSA/Fg adsorption versus the deposited PDA response.

3.2 Nonspecific protein adsorption and cell adhesion on PDA coating

We examined the nonspecific protein adsorption on the PDA coatings with gradient thicknesses by a sensitive, reliable and real-time SPR technique. As shown in Fig. 3, the adsorbed amount of BSA and Fg increased almost linearly with the increase of the deposited PDA thickness. This phenomenon might firstly be related to the morphological change of PDA coating with increasing thickness. As shown in Fig. 4, denser and bigger topographical features appeared along with the extended dip-coating time and the corresponding R_q roughness increased significantly, implying that the surface area of PDA coating grew with the increasing thickness. The increased surface area provided more binding sites for proteins.

Furthermore, the PDA coating-thickness-dependent protein adsorption can be correlated with the molecular structure and functional groups of PDA coating. Although PDA was widely used as active coatings, the molecular mechanisms allowing for the deposition of PDA films was still uncertain. Whereas, it is certain that a number of hydroxyl, amine groups and benzene rings exist in the PDA coating, possibly including π–π stacking structures[25,51,52]. These structural features contribute a lot to the adsorption of protein on account that they serve as binding sites to react with amine- or thiol- functionalized molecules via Schiff-base or Michael addition chemistry. The increase of PDA thickness is accompanied by the accumulation of active points to react with proteins, resulting in the linear increase of both BSA and Fg adsorption amounts with the increase of PDA thickness.

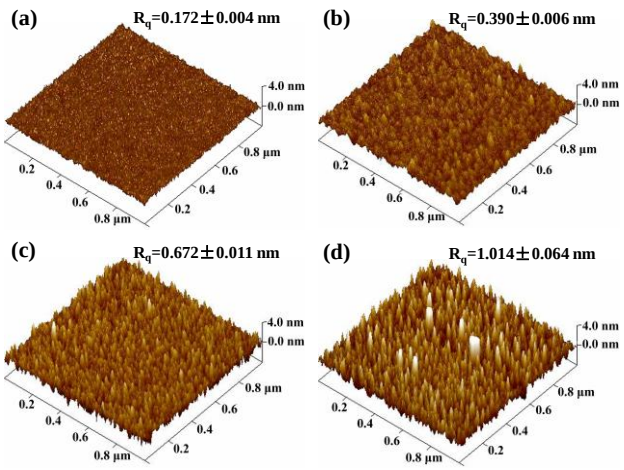

Fig. 4 AFM 3D images of PDA coated Si wafers with different immersion time in 2 mg/ml dopamine Tris/HCl (pH 8.5) buffer. (a) Bare Si wafer; (b) PDA deposited for 30 min; (c) PDA deposited for 3 hours; (d) PDA deposited for 6 hours.

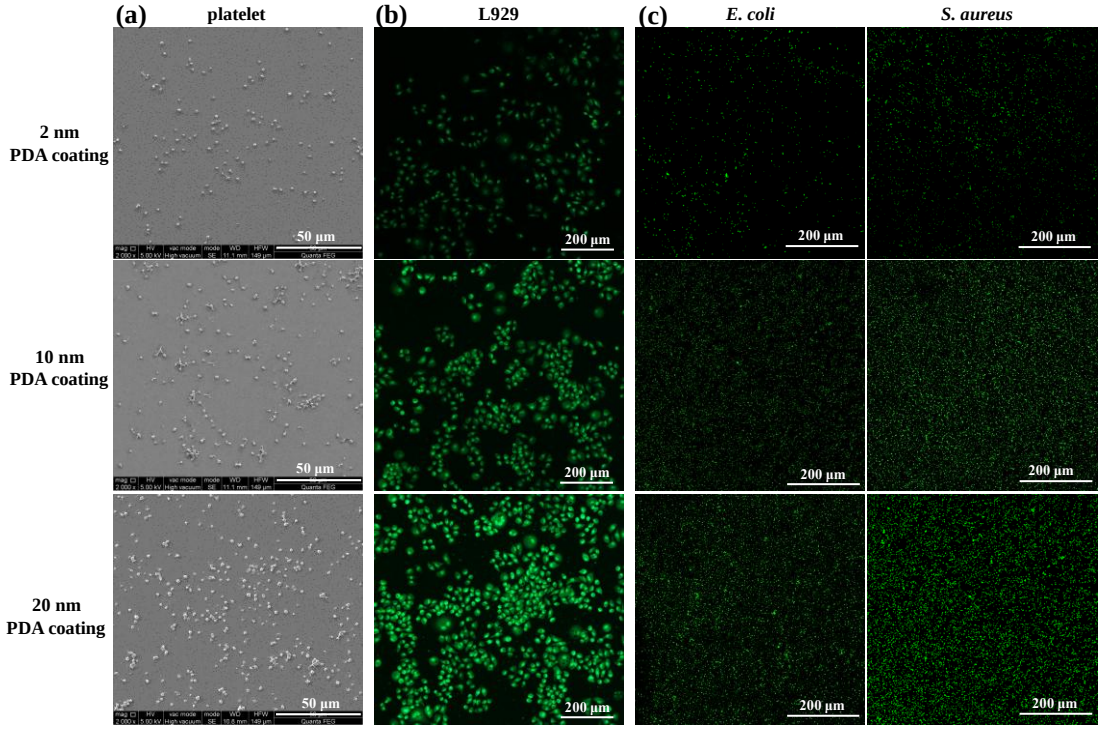

Fig. 5 (a) SEM images of adhered platelets, (b) Inverted fluorescence microscopic images of attached L929 fibroblast cells, (c) CLSM fluorescence microscopic images of attached *E. coli* and *S. aureus* on PDA coatings with different thicknesses. The tested coatings were prepared by immersing clean glass substrates in 2 mg/ml dopamine Tris/HCl (pH 8.5) buffer for 30 min, 3 hours or 6 hours, and then thoroughly rinsed with Millipore water and dried with nitrogen before using.

The rapid increase part of BSA protein adsorption with the increasing thickness of PDA coating could be explained as follows. When the SPR response was below 2000 μRIU, the gold surface might not be fully covered by PDA coating. The exposed small bare gold sites facilitated the BSA adsorption faster than that of Fg. Since the smaller BSA can enter the coating deficiency easily than the bigger Fg, the adsorption of BSA could be the combined result of gold substrate and PDA coating, while Fg adsorption might be merely induced by PDA coating. After the full-scale covered PDA coating (thicker than 2000 μRIU) was formed, PDA coating became the main induction for BSA and Fg adsorption, leading to their similar increasing trend.

From the PDA coating-thickness-dependent result of protein adsorption, we predicted that thicker PDA coating would induce more biofoulants to be adhered. The PDA coated glass substrates with different thicknesses were further tested by contact with platelet, L929 fibroblast cell, Gram positive and negative strains of *S. aureus* and *E. coli*, to verify the aforementioned prediction. Based on the SPR results shown in Fig. 2(c), the thicknesses of the PDA coatings deposited for 30 min, 3 hours and 6 hours were roughly 2 nm, 10 nm and 20 nm, respectively. As shown in Fig. 5, the attached platelet, L929 fibroblast cells and bacteria on 20 nm thick PDA coatings obviously outnumbered those on 2 nm and 10 nm PDA coatings. Similarly, the 10 nm PDA coating attracted more biofoulants (platelet, L929 fibroblast cells, *E. coli* and *S. aureus*) as compared to the 2 nm PDA coating. These results were in good consistence with the report of Ku and Park, and they found highly enhanced adhesion of endothelial cells on polycaprolactone nanofiber scaffold coated with a thick PDA film.[33] Based on the above results, we questioned whether the pristine dip-coated PDA coating could be directly utilized as a surface modifier for blood-contacting materials.

3.3 PDA coating modification strategies

The increased biofouling of a thick PDA coating may be attributed to the accumulation of free $–NH_2$, –NH– and –OH functional groups within the PDA coating, which provides abundant combining sites for biomolecules or microorganisms via Schiff-base reaction, Michael addition chemistry or intermolecular interactions. Therefore, changing the group composition of PDA surface may provide an effective way to reduce biofouling of PDA coatings. The functional groups in PDA matrix including quinone, carboxy-, amino-, imine-, and phenol groups could coordinate with multivalent metal ions[53], forming a catechol-M^{n+} complexation network. In addition, further oxidation and cross-linking of PDA coating by oxidants[54] or heating treatment[55] would decrease the concentration of free $–NH_2$, –NH– and –OH groups, probably paving another way to control the adsorption/adhesion of biofoulants.

For proof-of-concept, we injected $FeCl_3$, $NaIO_4$ solutions through PDA (thickness of 10000 ± 500 μRIU, about 10 nm)

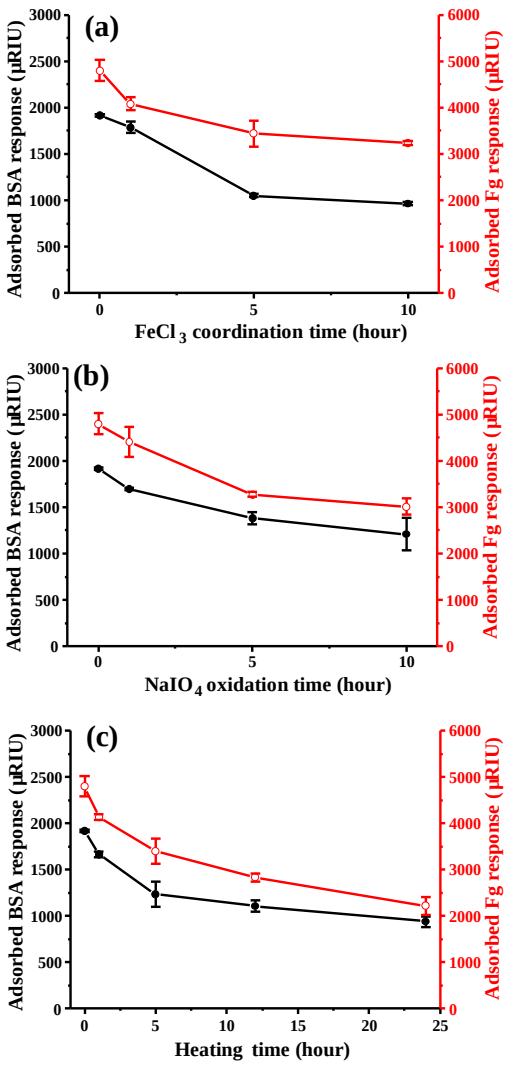

Fig. 6 Plots of SPR responses from BSA/Fg adsorption on differently treated PDA coatings versus the treatment time. The 10 nm thick PDA coating on the chips were treated by (a) passing 0.01 mg/ml $FeCl_3$ for specific times at a flow rate of 5 μl/min; (b) passing 0.01 mg/ml $NaIO_4$ for specific times at a flow rate of 5 μl/min; (c) 130°C treating for specific times in air.

coated SPR chips for specific periods at a flow rate of 5 μl/min, or heating the 10 nm thick PDA coated SPR chips at 130 ℃ in air for different times. Nonspecific protein adsorption on the Fe^{3+} chelated, $NaIO_4$ oxidized or heated PDA coatings was evaluated by sensitive and reliable SPR technique. As shown in Fig. 6, such treated PDA coatings suppressed 32~54% of BSA and Fg adsorption as compared to the virgin PDA coating. Interestingly, the protein adsorption was suppressed by more than 50% for the simple heating treatment. This result is possibly due to more extensive oxidation and cross-linking within the PDA coating by the heating treatment.

Represented by the thermally treated PDA coating, we analysed the characteristic group changes of PDA coatings before and after the heating treatment by ATR-FTIR spectroscopy and XPS measurements. ATR-FTIR spectra (Fig. 7(a)) illustrated that both the heated and unheated PDA coated PP surfaces had a broad peak in the range of 3100~3600 cm^{-1}, which could be ascribed to aromatic protons, $-NH_2$, –NH– and –OH group stretching vibrations. Compared to the broad adsorption of frame vibration of benzene ring at 1620 cm^{-1} of unheated PDA coating, the thermally treated PDA coating showed distinct signals at 1742 cm^{-1} (O–C=O stretching vibration), 1640 cm^{-1} (C=O stretching vibration) and 1555 cm^{-1} ($-NO_2$ asymmetric stretching vibration), suggesting that the heating treatment changed the surface chemical groups. Furthermore, the slight decrease in peak intensity in the range of 3100~3600 cm^{-1} might also be ascribed to the decreased number of $-NH_2$, –NH– and –OH groups on the heated PDA coating.

To confirm the ATR-FTIR result by more solid evidence, chemical compositions of the unheated and heated PDA coatings were analysed by measuring high resolution XPS spectra. Referring to published binding styles of PDA coating[32, 55-57], we obtained the high-resolution C1s and N1s XPS spectra as shown in Fig. 7(b). Compared to the unheated PDA coating, the obviously increased peak at 288.2 eV (C=O) and newly appeared peak at 407.1 eV ($-NO_x$) in C1s and N1s high resolution spectra of the heated PDA coating, suggested that the oxidation of surface chemical groups occurred after 130 ℃

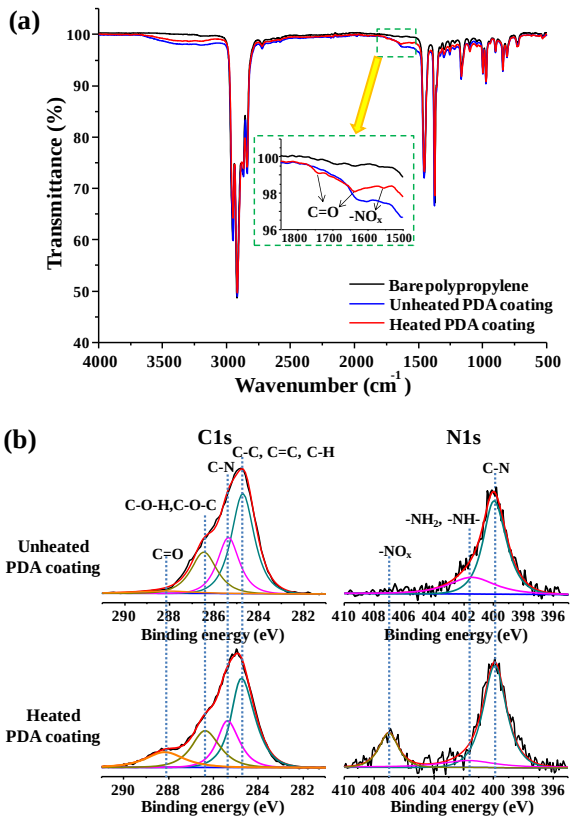

Fig. 7 (a) ATR-FTIR spectra of unheated and heated PDA coatings on PP substrates. (b) High resolution C1s and N1s XPS spectra of unheated and heated PDA coatings on glass substrates. The coatings were prepared by immersing PP/glass slide in freshly prepared dopamine solutions (2 mg/ml in 10 mM Tris/HCl buffer at pH 8.5) for 3 hours. After thoroughly rinsing the PDA coated substrates with Millipore water and drying under a stream of nitrogen. A portion of these PDA coatings were heated at 130°C in air for 12 hours and were characterized under the same condition with the unheated PDA coatings.

Table 1 The contents of differently bound C and N obtained by curve fitting of the high resolution C1s and N1s XPS spectra of PDA coatings.

Sample	C1s (%)				N1s (%)		
	C-C, C=C, C-H	C-N	C-O-H, C-O-C	C=O	C-N	$-NH_2$, -NH-	$-NO_2$
Unheated PDA coating	48.1	25.7	22.6	3.5	74.0	26.0	–
Heated PDA coating	44.3	21.8	21.7	12.2	70.5	10.0	19.5

heating for 12 hours. Furthermore, the contents of differently bound C and N were analyzed and listed in Table 1. The pristine PDA coating had 3.5% C=O and 0% $-NO_x$, while the C=O and $-NO_x$ contents of thermally treated PDA coating increased to 12.2% and 19.5%. Meanwhile, the contents of $-NH_2$, –NH–, C–C, C=C, C–H and C–O–H groups decreased after the thermal treatment in air. Obviously, the increase of C=O and $-NO_x$ groups was accompanied by the decrease of $-NH_2$, –NH–, –OH and C–H groups, implying that the reactive groups ($-NH_2$, –NH– and –OH) were transformed to inert groups ($-NO_x$, C=O and C–O) after heating the PDA coating.

Based on the protein adsorption and chemical composition results, we predicted that lowering the surface contents of reactive $-NH_2$, –NH– and –OH groups would effectively suppress the adsorption/adhesion of biofoulants to some extent.[58] However, the benzene rings and possible π–π stacking structure of PDA coating[51] couldn't be completely eliminated and might attract biofoulants via hydrophobic and conjugate interactions. Consequently, PDA coating itself may not be an ideal blood-contacting interface in surface modification.

On the other hand, the rich amino and catechol groups in PDA coating provide a versatile platform for further modification with antifouling polymers. In this study, we synthesized a zwitterionic copolymer PMEN bearing cell membrane anti-fouling phosphorylcholine and *p*-nitrophenyl active ester groups. The phosphorylcholine polymer was fixed on the PDA coating via the amidation coupling between the amino groups of PDA coating and the active ester groups in PMEN by forming amide bond and releasing *p*-nitrophenol.

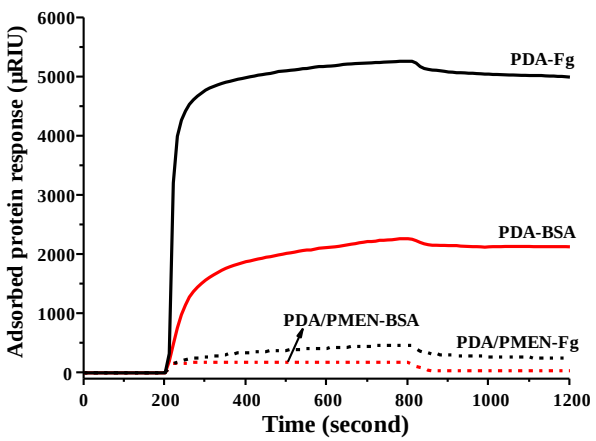

Fig. 8 Typical SPR sensorgrams of BSA and Fg adsorption on PDA and PDA/PMEN coatings. The PDA/PMEN coating was constructed by injecting PMEN ethanol solution (2 mg/ml) through 10 nm PDA precoated gold chips in situ for 5 hours at a flow rate of 5 μl/min.

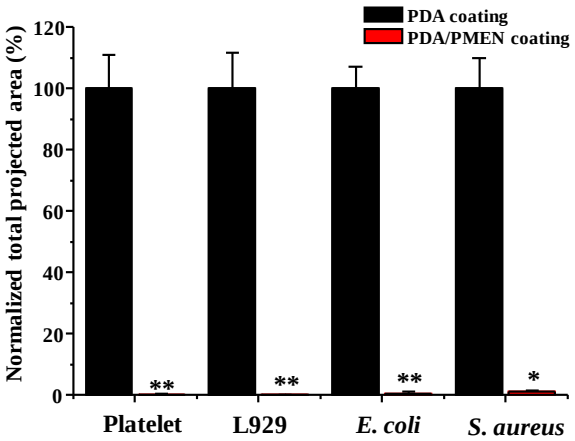

Fig. 9 Quantitative results of platelet, L929, *E. coli* and *S. aureus* adhesion on pristine and PMEN grafted 10 nm PDA coating surfaces obtained by threshold analysis with ImageJ. The surfaces were prepared by immersing glass substrates in freshly prepared dopamine solutions (2 mg/ml in 10 mM Tris/HCl buffer at pH 8.5) for 3 hours. After thoroughly rinsing the PDA coated substrates with Millipore water, the PDA precoated glass was transferred into 5 mg/ml PMEN in ethanol and grafted at 60°C for 5 hours. *$p \leq 0.05$ and **$p \leq 0.01$.

Gong *et al* reported that the amidation efficiency between these two groups was approximately 100%.[59] ATR-FTIR and high resolution N1s and P2p XPS analysis results (Fig. S2) confirmed the successful coupling of the PMEN film on PDA coated glass substrates and suggested complete masking of the PDA surface. As shown in Fig. 8, the formed PDA/PMEN coating resisted 98.6% and 95.9% of protein adsorption for BSA and Fg compared to that of the 10 nm thick PDA coating. In addition to this excellent anti-protein adsorption behaviour, much better anti-adhesion performance for cells and pathogenic bacteria was demonstrated in Fig. S3 and the quantitative results were shown in Fig. 9. More than 99% of platelet, L929 and bacteria fouling are effectively suppressed on PDA/PMEN surfaces in comparison with that on the 10 nm thick PDA coating. The excellent anti-biofouling performance of this simply self-anchoring PDA/PMEN coating, is as good as that of chemically grafted zwitterionic polymer brushes prepared by complicated processes.[60] Its exciting anti-biofouling result can be ascribed to the total replacement/masking of the amino and catechol groups on coating surface by zwitterionic phosphorylcholine groups.[42, 59-63]

The possible changes in surface chemical components of PDA coatings by different treatments were schematically illustrated in Scheme 1. All the simple treatments of PDA coating caused changes in the group composition of the surfaces. The decrease of reactive $-NH_2$, –NH– and –OH groups could effectively suppress the adsorption/adhesion of

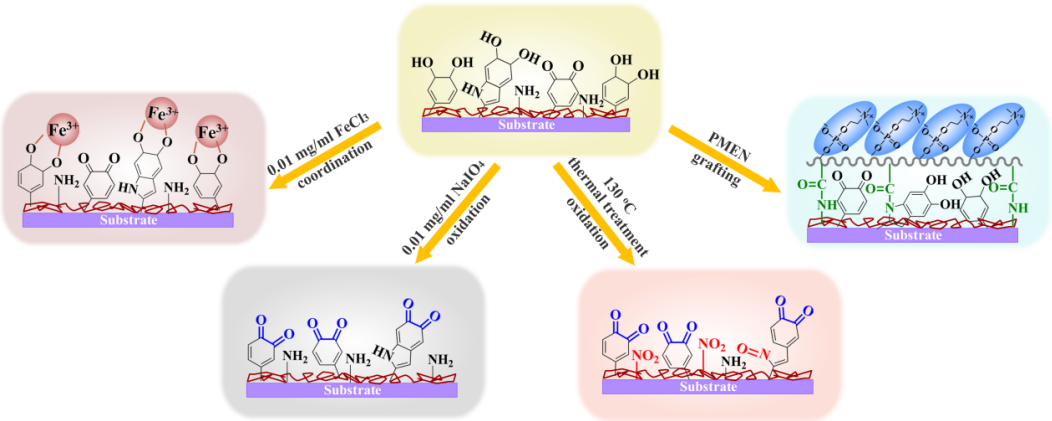

Scheme 1 Schematic illustration of chemical component changes of PDA coatings after different treatments.

biofoulants to some extent. However, protein adsorption on PDA coatings treated by $FeCl_3$ coordination, $NaIO_4$ oxidation and heating might be still higher than the threshold value that triggering platelet activation and thrombin.[64] In order to satisfy the highest standard of blood-contacting surface, cell outer membrane mimetic phosphorylcholine copolymer PMEN covered PDA coating (PDA/PMEN) could be a versatile strategy, since such a coating might be formed automatically in aqueous solution on substrate independent surface under mild conditions.

4 Conclusions

The SPR real-time investigation of PDA coating formation under different pH, initial dopamine concentration and deposition time provided more details to construct a well controlled PDA coating. A series of PDA coatings with gradient thicknesses were fabricated and their anti-biofouling performance was evaluated. The increased nonspecific protein adsorption with the increasing PDA thickness could be ascribed to the accompanied accumulation of reactive functional groups within the PDA matrix. The results of platelet, L929 fibroblast cells and bacteria adhesions on PDA coatings with different thicknesses supported the finding of thickness-dependent biofouling attachment. The PDA coating was further treated by $FeCl_3$ coordination, $NaIO_4$ oxidation and heating and the protein adsorption was effectively suppressed. Furthermore, a cell membrane mimetic phosphorylcholine copolymer PMEN was grafted on the PDA surface by immersion coating. The resulted PDA/PMEN surface showed excellent resistance to protein adsorption, platelet, L929 fibroblast and bacteria adhesions. Overall, the anti-biofouling performance of PDA coating is limited, but can be improved significantly by simple coordination, oxidation and heating treatments. Moreover, excellent anti-biofouling can be obtained by simply coating a cell membrane mimetic phosphorylcholine polymer containing active ester group. This substrate-independent, simple two-step surface coating strategy may find applications in the vast area of surface antifouling, especially for most biomedical devices.

Acknowledgements

This work was supported by the National Natural Science Foundation of China (Nos. 21244001, 21374087), and the Fund of Engineering Laboratory of Xi'an City (No. 2012-12).

Notes and references

Key Laboratory of Synthetic and Natural Functional Molecule Chemistry of Ministry of Education, College of Chemistry and Materials Science, Northwest University, Xi'an 710127, Shaanxi, PR China. Email: gongyk@nwu.edu.cn, Tel: (86) 29 81535032, Fax: (86) 29 81535026.

† Electronic Supplementary Information (ESI) available: ^{1}H NMR spectra of PMEN copolymer (Fig. S1), ATR-FTIR and XPS survey spectra of PDA/PMEN and PDA coated substrates (Fig. S2), images of adherent platelets, L929 fibroblast cells, *E. coli* and *S. aureus* on PDA/PMEN and PDA coatings. See DOI: 10.1039/b000000x/.

1 S. Jiang and Z. Cao, *Adv. Mater.*, 2010, **22**, 920.
2 Y. Liu, K. Ai and L. Lu, *Chem. Rev.*, 2014, **114**, 5057.
3 Z. Yang, J. Wang, R. Luo, M. F. Maitz, F. Jing, H. Sun and N. Huang, *Biomaterials*, 2010, **31**, 2072.
4 J. Wang, B. Li, Z. Li, K. Ren, L. Jin, S. Zhang, H. Chang, Y. Sun and J. Ji, *Biomaterials*, 2014, **35**, 7679.
5 P. Liu, Q. Chen, L. Li, S. Lin and J. Shen, *J. Mater. Chem. B*, 2014, **2**, 7222.
6 A. J. Blok, R. Chhasatia, J. Dilag and A. V. Ellis, *J. Membrane Sci.*, 2014, **468**, 216.
7 L. Xu, P. Ma, B. Yuan, Q. Chen, S. Lin, X. Chen, Z. Hua and J. Shen, *RSC Adv.*, 2014, **4**, 15030.
8 S. Y. Park, J. W. Chung, Y. K. Chae and S. Kwak, *ACS Appl. Mater. Inter.*, 2013, **5**, 10705.
9 H. Yin, T. Akasaki, T. Lin Sun, T. Nakajima, T. Kurokawa, T. Nonoyama, T. Taira, Y. Saruwatari and J. P. Gong, *J. Mater. Chem. B*, 2013, **1**, 3685.

10 K. A. Pollack, P. M. Imbesi, J. E. Raymond and K. L. Wooley, *ACS Appl. Mater. Inter.*, 2014, **6**, 19265.
11 K. L. Prime and G. M. Whitesides, *Science*, 1991, **252**, 1164.
12 G. Cheng, H. Xue, Z. Zhang, S. Chen and S. Jiang, *Angew. Chem. Int. Ed.*, 2008, **47**, 8831.
13 W. Lin, G. Ma, F. Ji, J. Zhang, L. Wang, H. Sun and S. Chen, *J. Mater. Chem. B*, 2015, **3**, 440.
14 N. Y. Kostina, S. Sharifi, A. de Los Santos Pereira, J. Michalek, D. W. Grijpma and C. Rodriguez-Emmenegger, *J. Mater. Chem. B*, 2013, **1**, 5644.
15 S. Chen and S. Jiang, *Adv. Mater.*, 2008, **20**, 335.
16 R. Zhou, P. Ren, H. Yang and Z. Xu, *J. Membrane Sci.*, 2014, **466**, 18.
17 W. Zhao, Q. Ye, H. Hu, X. Wang and F. Zhou, *J. Mater. Chem. B*, 2014, **2**, 5352.
18 D. Tan, Z. Li, X. Yao, C. Xiang, H. Tan and Q. Fu, *J. Mater. Chem. B*, 2014, **2**, 1344.
19 A. J. Morse, S. Edmondson, D. Dupin, S. P. Armes, Z. Zhang, G. J. Leggett, R. L. Thompson and A. L. Lewis, *Soft Matter*, 2010, **6**, 1571.
20 H. Lee, S. M. Dellatore, W. M. Miller and P. B. Messersmith, *Science*, 2007, **318**, 426.
21 W. Tsai, C. Chien, H. Thissen and J. Lai, *Acta Biomater.*, 2011, **7**, 2518.
22 B. P. Lee, C. Chao, F. N. Nunalee, E. Motan, K. R. Shull and P. B. Messersmith, *Macromolecules*, 2006, **39**, 1740.
23 J. Wang, B. Li, Z. Li, K. Ren, L. Jin, S. Zhang, H. Chang, Y. Sun and J. Ji, *Biomaterials*, 2014, **35**, 7679.
24 F. Bernsmann, V. Ball, F. Addiego, A. Ponche, M. Michel, J. J. D. A. Gracio, V. Toniazzo and D. Ruch, *Langmuir*, 2011, **27**, 2819.
25 S. Hong, Y. S. Na, S. Choi, I. T. Song, W. Y. Kim and H. Lee, *Adv. Funct. Mater.*, 2012, **22**, 4711.
26 Q. Ye, F. Zhou and W. Liu, *Chem. Soc. Rev.*, 2011, **40**, 4244.
27 H. Lee, N. F. Scherer and P. B. Messersmith, *Proc. Natl. Acad. Sci. USA*, 2006, **103**, 12999.
28 C. Gao, G. Li, H. Xue, W. Yang, F. Zhang and S. Jiang, *Biomaterials*, 2010, **31**, 1486.
29 Y. Yang, P. Qi, Y. Ding, M. F. Maitz, Z. Yang, Q. Tu, K. Xiong, Y. Leng and N. Huang, *J. Mater. Chem. B*, 2015, **3**, 72.
30 S. M. Kang, N. S. Hwang, J. Yeom, S. Y. Park, P. B. Messersmith, I. S. Choi, R. Langer, D. G. Anderson and H. Lee, *Adv. Funct. Mater.*, 2012, **22**, 2949.
31 J. Wang, K. Ren, H. Chang, S. Zhang, L. Jin and J. Ji, *Phys. Chem. Chem. Phys.*, 2014, **16**, 2936.
32 S. H. Ku, J. Ryu, S. K. Hong, H. Lee and C. B. Park, *Biomaterials*, 2010, **31**, 2535.
33 S. H. Ku and C. B. Park, *Biomaterials*, 2010, **31**, 9431.
34 S. Hong, K. Y. Kim, H. J. Wook, S. Y. Park, K. D. Lee, D. Y. Lee and H. Lee, *Nanomedicine*, 2011, **6**, 793.
35 Y. Liu, K. Ai, J. Liu, M. Deng, Y. He and L. Lu, *Adv. Mater.*, 2013, **25**, 1353.
36 X. Liu, J. Cao, H. Li, J. Li, Q. Jin, K. Ren and J. Ji, *ACS Nano*, 2013, **7**, 9384.
37 H. Karkhanechi, R. Takagi and H. Matsuyama, *Desalination*, 2014, **336**, 87.
38 B. D. McCloskey, H. B. Park, H. Ju, B. W. Rowe, D. J. Miller and B. D. Freeman, *J. Membrane Sci.*, 2012, **82**, 413.
39 Z. Yang, S. Zhong, Y. Yang, M. F. Maitz, X. Li, Q. Tu, P. Qi, H. Zhang, H. Qiu, J. Wang and N. Huang, *J. Mater. Chem. B*, 2014, **2**, 6767.
40 Y. Yang, P. Qi, F. Wen, X. Li, Q. Xia, M. F. Maitz, Z. Yang, R. Shen, Q. Tu and N. Huang, *ACS Appl. Mater. Inter.*, 2014, **6**, 14608.
41 Y. Weng, Q. Song, Y. Zhou, L. Zhang, J. Wang, J. Chen, Y. Leng, S. Li and N. Huang, *Biomaterials*, 2011, **32**, 1253.
42 Y. Dang, M. Quan, C. Xing, Y. Wang and Y. Gong, *J. Mater. Chem. B*, 2015, **3**, 2350.
43 K. Ishihara, T. Ueda and N. Nakabayashi, *Polym. J.*, 1990, **22**, 355.
44 T. Konno, J. Watanabe and K. Ishihara, *Biomacromolecules*, 2004, **5**, 342.
45 A. L. Lewis, H. P. D, L. C. Kirkwood, S. W. Leppard, R. P. Redman, L. A. Tolhurst and P. W. Stratford, *Biomaterials*, 2000, **21**, 1847.
46 M. Gong, Y. Wang, M. Li, B. Hu and Y. Gong, *Colloids Surf. B*, 2011, **85**, 48.
47 D. E. Fullenkamp, J. G. Rivera, Y. Gong, K. H. A. Lau, L. He, R. Varshney and P. B. Messersmith, *Biomaterials*, 2012, **33**, 3783.
48 M. Tanaka, T. Sawaguchi, Y. Sato, K. Yoshioka and O. Niwa, *Tetrahedron Lett.*, 2009, **50**, 4092.
49 V. Ball, D. D. Frari, V. Toniazzo and D. Ruch, *J. Colloid Interf. Sci.*, 2012, **386**, 366.
50 F. Bernsmann, A. Ponche, C. Ringwald, J. Hemmerle, J. Raya, B. Bechinger, J. Voegel, P. Schaaf and V. Ball, *J. Phys. Chem. C*, 2009, **113**, 8234.
51 D. R. Dreyer, D. J. Miller, B. D. Freeman, D. R. Paul and C. W. Bielawski, *Langmuir*, 2012, **28**, 6428.
52 J. Liebscher, R. Mrówczyński, H. A. Scheidt, C. Filip, N. D. Hădade, R. Turcu, A. Bende and S. Beck, *Langmuir*, 2013, **29**, 10539.
53 M. D'Ischia, A. Napolitano, A. Pezzella, P. Meredith and T. Sarna, *Angew. Chem. Int. Ed.*, 2009, **48**, 3914.
54 V. Ball, I. Nguyen, M. Haupt, C. Oehr, C. Arnoult, V. Toniazzo and D. Ruch, *J. Colloid Interf. Sci.*, 2011, **364**, 359.
55 J. Jiang, L. Zhu, X. Li, Y. Xu and B. Zhu, *J. Membrane Sci.*, 2010, **364**, 194.
56 M. B. Clark, J. A. Gardella, T. M. Schultz, D. G. Patil and L. A. C. Salvati, *Anal. Chem.*, 1990, **62**, 949.
57 L. Q. Xu, W. J. Yang, K. Neoh, E. Kang and G. D. Fu, *Macromolecules*, 2010, **43**, 8336.
58 R. Luo, L. Tang, S. Zhong, Z. Yang, J. Wang, Y. Weng, Q. Tu, C. Jiang and N. Huang, *ACS Appl. Mater. Inter.*, 2013, **5**, 1704.
59 Y. Gong, L. Liu and P. B. Messersmith, *Macromol. Biosci.*, 2012, **12**, 979.
60 J. Kuang and P. B. Messersmith, *Langmuir*, 2012, **28**, 7258.
61 Y. Wang, M. Gong, S. Yang, K. Nakashima and Y. Gong, *J. Membrane Sci.*, 2014, **452**, 29.
62 N. Hao, Y. Wang, S. Zhang, S. Shi, K. Nakashima and Y. Gong, 2014, **102**, 2972.
63 M. Gong, Y. Dang, Y. Wang, S. Yang, F. M. Winnik and Y. Gong, *Soft Matter*, 2013, **9**, 4501.
64 K. Park, F. W. Mao and H. Park, *J. Biomed. Mater. Res.*, 1991, **25**, 407.

Table of Contents

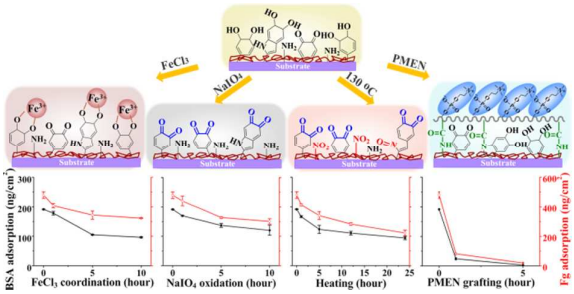

Anti-biofouling performance of mussel inspired polydopamine coating can be improved significantly by simple coordination, oxidation, heating or grafting treatment.